AN ABSTRACT OF THE THESIS OF

Elham Bagherisereshki for the degree of Master of Science in Chemical Engineering presented on May 25, 2016.

Title: Carbonation Kinetics of SrO By CO_2 for Solar Thermochemical Energy Storage

Abstract approved:

_____

Nicholas J. AuYeung

Given its abundance and accessibility, exploiting solar energy is a powerful approach to reduce dependency on fossil fuels for energy generation. Thermochemical reactions using concentrated solar power at high temperature are an attractive method of energy storage in support of concentrated solar power (CSP). Thermochemical energy storage of on-sun thermal energy is achieved when a reactive system absorbs thermal energy and proceeds with a reversible chemical reaction. In a time of power demand, the reverse reaction is then initiated and energy is released, thus recovering stored chemical energy for use in a power cycle .In this study, strontium-oxide (SrO) carbonation kinetics have been studied by means of thermogravimetric analysis (TGA) and a laboratory scale apparatus including a tube furnace packed with SrO particles dispersed in sand for thermochemical energy storage. In order to better describe the reaction mechanism, the influence of intensive variables such as reaction temperature and CO_2 partial pressure were investigated. In both methods, carbonation was performed at several temperatures (900-1150°C) under isothermal conditions. The effect of sample size (25 – 106 μm) and partial pressures of CO_2 (0.1-1 bar) has been investigated in

TGA. The carbonation reaction progression obtained from TGA can be divided into three stages: an initial induction period; a rapid kinetically-controlled carbonation stage; and finally a sluggish diffusion-controlled regime. The existence of a true induction period must be investigated in an experimental apparatus other than a TGA. The carbonation conversion result from the laboratory scale fixed bed do not indicate the existence of this time period.

Time-dependent carbonation conversion after removing the induction period appeared as sigmoid curves. The conversion rates of SrO carbonation were well fitted to Lee's model for the carbonation reaction of calcium oxide by carbon dioxide. The reaction rate constant k as a temperature dependent term presented by Arrhenius equation with activation energy of E_a = 12.02 kJ.mol^{-1} and the pre-exponential factor of A = 0.323 min^{-1} for TGA.

Carbonation Kinetics of SrO By CO_2 for Solar Thermochemical Energy Storage

by
Elham Bagherisereshki

A THESIS

submitted to

Oregon State University

in partial fulfillment of
the requirements for the
degree of

Master of Science

Presented May 25, 2016
Commencement June 2016

Master of Science thesis of Elham Bagherisereshki presented on May 25, 2016

APPROVED:

Major Professor, representing Chemical Engineering

Head of the School of Chemical, Biological, and Environmental Engineering

Dean of the Graduate School

I understand that my thesis will become part of the permanent collection of Oregon State University libraries. My signature below authorizes release of my thesis to any reader upon request.

Elham Bagherisereshki, Author

TABLE OF CONTENTS

Page

LIST OF FIGURES

Figure Page

LIST OF TABLES

Table Page

Carbonation Kinetics of SrO By CO_2 for Solar Thermochemical Energy Storage

1. Introduction

Concentrated solar power (CSP) is one promising method of converting clean solar thermal energy into electricity which avoids the use of fossil fuels and the anthropogenic greenhouse effect. [1,2] CSP in conjunction with thermal energy storage (TES) can increase the utilization of solar energy by enabling plant operators to generate electricity beyond normal on-sun hours thus can be a more efficient and cost-effective technology than photovoltaic (PV) technologies that directly convert solar energy directly into electricity. Thermochemical energy storage (TCES) is an emerging type of TES system based on a reversible reaction that offers greater volumetric and gravimetric energy density than latent or sensible energy storage. Efficiency of a power generation system depends on the temperature at which heat is available and the temperature level at which the reject heat can be disposed according to the second law of thermodynamics and Carnot efficiency. Thus, high efficiency is reached by energy release at high temperature that is attainable with TCES systems. Moreover, the capital cost of thermal energy storage subsystems is reduced with greater volumetric energy density. Thermochemical energy storage of on-sun thermal energy is achieved when a reactive system absorbs thermal energy and proceeds with a reversible chemical reaction. In a time of power demand, the reverse reaction is then initiated and energy is released, thus recovering stored chemical energy for use in a power cycle. [3,4]

Recently, a review focusing on high temperature [300-1000°C] thermochemical heat energy storage has been published. Different TCES systems have been classified according to their reaction family. Metallic hydrides, carbonates, hydroxides, redox system, ammonia system and organic system such as CH_4/H_2O, CH_4/CO_2 are candidates for high-temperature thermochemical heat energy storage. Among these candidates, the ammonia dissociation and synthesis is the most developed system which has been tested at the pilot–scale, while most of other systems have only been tested on a laboratory scale. Moreover, the dehydration/hydration of the $Ca(OH)_2/CaO$ couple has been studied as a potential system for energy storage, but additional studies and projects must be done to overcome different barriers hindering scale-up. [5]

CaO precursors are cheap and widely available which make carbonation/decomposition cycling of $CaCO_3/CaO$ suitable for a variety of uses such as thermochemical energy storage, pre-combustion and post-combustion CO_2 capture. [6–10] The reversible calcium looping cycle between CaO and $CaCO_3$ occurs between 650 and 900 ºC, at atmospheric pressure. [7,9]

$$CaCO_3 \leftrightarrow CaO + CO_2 \qquad \Delta H^{\circ}_{rxn,25^{\circ}C} = 178.4 kJmol^{-1} \qquad (1)$$

CaO-based sorbents exhibit a great capacity for CO_2 adsorption, however like most sorbents, this capacity eventually reduces with the number of carbonation/calcination cycles. [8]

An energy storage system similar to $CaO/CaCO_3$ based on the reversible carbonation/decomposition of $SrO/SrCO_3$, has been introduced by Arlt and Wasserschield. [11]

$$SrCO_3 \leftrightarrow SrO + CO_2 \qquad \Delta H^{\circ}_{rxn,25^{\circ}C} = 234 kJmol^{-1} \qquad (2)$$

Under atmospheric pressure, the cyclic carbonation/decomposition occurs at high temperatures (≈ 1200°C). Such high-quality heat is suitable for high efficiency, combined cycle power generation, which has the potential to translate into more competitive solar electricity prices. The endothermic decomposition of $SrCO_3$ occurs at a temperature greater than the equilibrium temperature ($\Delta G^{\circ} = 0$ kJ mol^{-1} at 1175°C). The reverse exothermic carbonation of SrO occurs at a temperature below the decomposition temperature and the released heat is used for power generation.

The common problems of such storage schemes are sintering and loss of surface area due to high-temperature involvement which slows down the reaction rate. The energy density of the system supported by zirconia-based sintering inhibitors was investigated by Rhodes et al.[4] In this investigation, samples of SrO with inert support material of yttria-stabilized strontium zirconate show energy densities of 1500, 1430 and 1260 MJ m^{-3} after 10, 15 and 45 cycles, respectively. In each cycle, the carbonation was conducted at 1150°C and the decomposition at 1235°C. Many operational and material synthesis parameters still need to be investigated in order to produce SrO samples which demonstrate stable energy density over many cycles.

Compared to other TCES candidate chemistries, there are significant advantages in energy storage using the $SrCO_3$/SrO system. The reaction does not involve any catalyst and there are no side reactions or side products. CO_2 is neither flammable nor corrosive, and moreover, it is non-toxic in low concentration. [4,12]

Strontium carbonate has been studied previously as a reference material for Differential Thermal Analysis (DTA).[13,14] The thermal decomposition of orthorhombic (α-$SrCO_3$) and hexagonal (β-$SrCO_3$) strontium carbonate polymorphs has been studied by non-isothermal thermogravimetric analysis (TGA). The reaction was then modeled using the Kissinger equation and a kinetic function fitting method. The "kinetic triplet" of the activation energy, frequency factor and solid state kinetic model was determined. It is shown that the transformation of α-$SrCO_3$ to β-$SrCO_3$ causes the activation energy of the process to decrease from 255 to 227 $kJmol^{-1}$ and changes the reaction mechanism from interface controlled growth to a process with zero or decreasing nucleation rate.[15]

Table 1 Kinetic data related to the thermal decomposition of strontium carbonate[15].

$SrCO_3$ polymorph	***E_a*** **[kJ mol^{-1}]**	***A*** **[$\times 10^7$ s^{-1}]**	***n***
Orthorhombic α	255 ± 3	15.8 ± 4.3	1.8 ± 0.1
Hexagonal β	227 ± 4	8.4 ± 3	1.6 ± 0.1

In order to accurately design a reactor for this TCES system and predict the rate of heat generation it is important to understand the kinetics of strontium oxide carbonation, which has not been studied. Moreover, knowing the kinetics assists us with improving the CO_2 capture capacity of SrO and comparing SrO to other material for thermochemical energy storage. Our research aims to present the kinetic model which accurately explains the experimental data for the carbonation reaction.

The thermodynamics of the system highly depend on the partial pressure of CO_2.[4] Figure 1 illustrates the equilibrium partial pressure of CO_2 ($P_{CO_2,eq}$) during the carbonation-decomposition reaction shown in equation (2) at temperature between 900 °C and 1175 °. Calculation of the equilibrium partial pressure is equivalent to the calculation of the equilibrium constant (K) assuming first order reaction.[16]:

$$K = P_{CO_2,eq} = \exp(-\frac{\Delta G^{\circ}_{rxn}(T)}{RT}) \qquad (3)$$

In equation (3), $P_{CO_2,eq}$ is the equilibrium partial pressure of CO_2 from the decomposition of $SrCO_3$. $\Delta G^{\circ}_{rxn}(T)$ is the standard state Gibbs free energy change for the reaction, calculated from tabulated thermochemical data provided by Barin.[17] The trend in Figure 1 suggests that increasing the partial pressure of CO_2 at a constant temperature or decreasing the temperature at a constant partial pressure of CO_2 would result in more capture of CO_2 by SrO.

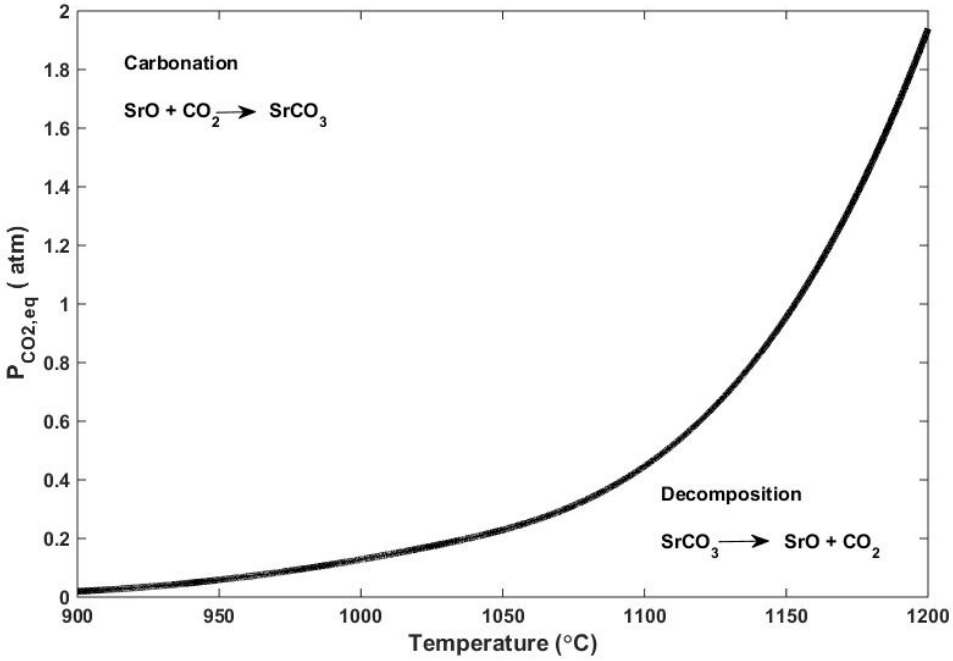

Figure 1 The equilibrium partial pressure of CO_2 resulting from the decomposition of $SrCO_3$

2. Experimental Section

2.1. Material Preparation

Strontium oxide (Alfa Aesar) was heated in a muffle furnace at 1500ºC for 8 h under air to ensure the formation of large grains. SrO powder absorbs moisture from the air and quickly transforms into $Sr(OH)_2$ or a hydrate during the material preparation process. Thus, the mass ratio of SrO is unknown at the beginning of the kinetic study. During the initial dehydration step at 1200°C in TGA, SrO is purified due to H_2O loss. The minimum mass reached after dehydration was taken to be the actual mass of SrO. The resulting powder was sieved to prepare samples in different particle size ranges: 25-53, 53-75, 75-106 µm. The specific surface area of the material was determined with the BET method using Micromeritics ASAP 2020. Table 2 gives the specific surface area, pore volume, and average pore diameter of the prepared SrO.

Table 2 Structural properties of SrO sorbent.

Sorbent	**Specific surface area (m^2/g)**	**Pore volume (ml/g)**	**Average pore diameter (Å)**
Strontium oxide	4.343	0.02457	226.338

2.2. Operation of the carbonation reaction in the TGA

Data were obtained by performing thermogravimetric analysis (TGA) using a TA instruments SDT Q600. For each experiment, approximately 40 mg of material was measured into an alumina crucible. As it is mentioned earlier, in the first step known, SrO samples were heated at 1200°C for 2 hours under an inert atmosphere (N_2) with a flow rate of 40 sccm. The temperature was then decreased at 5°C min^{-1} to the carbonation temperature, in the range 900 – 1150 °C and stabilized around 10 min before introducing CO_2 with the flow rate of 40 sccm to initiate the exothermic carbonation step. Figure 2 represents the mass and temperature change during a typical experiment with 40 mg of a sample at 1100 °C. All the carbonation reactions were performed in a similar fashion under isothermal conditions. Similarly, the effect of partial pressures of CO_2 (0.1-1 bar) has been investigated at 900 °C and 1000 °C.

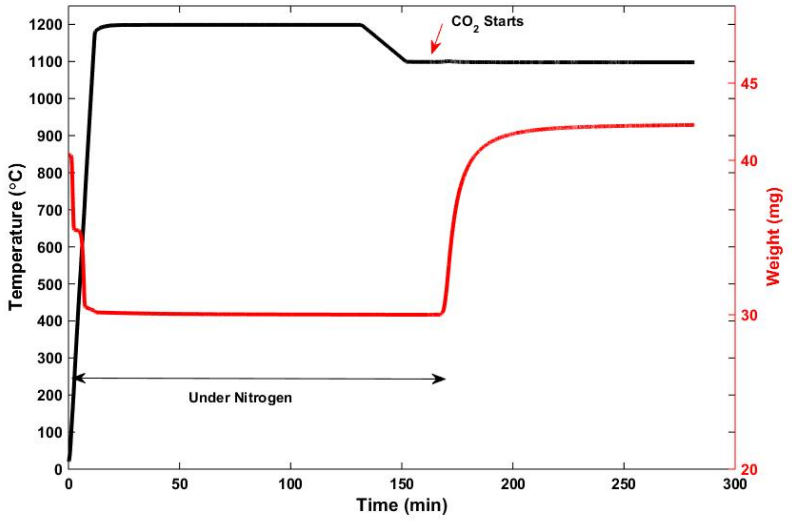

Figure 2 an experiment on TGA and typical shape of carbonation curves (carbonation at 1100°C under 1 bar in CO_2).

Plots of fractional conversion versus time were obtained from the measured mass changes:

$$X_{SrO} = \frac{m_t - m_0}{m_0} \frac{M_{SrO}}{M_{CO_2}} \qquad (4)$$

where m_0 is the initial SrO weight after complete dehydration, m_t is SrO weight at time t, and M_{CO_2} and M_{SrO} are molecular weights of SrO and CO_2 equal to 103.62 and 44.01 (g/mol), respectively.

A series of experiments was carried out to determine the effects of the particle size of SrO on carbonation reaction at 1100 °C and 1 bar of CO_2 pressure. Figure 3 shows that the particle size of SrO varying from less than 25 μm to more than 106 μm had almost no effect on the carbonation behavior. The carbonation behavior of SrO is independent of particle size. Therefore, the kinetic experiments were performed by using particles with a diameter of 53-75 μm. This might be the result of dehydration step at 1200°C, during which the particle size very well could equalize due to the high temperature.

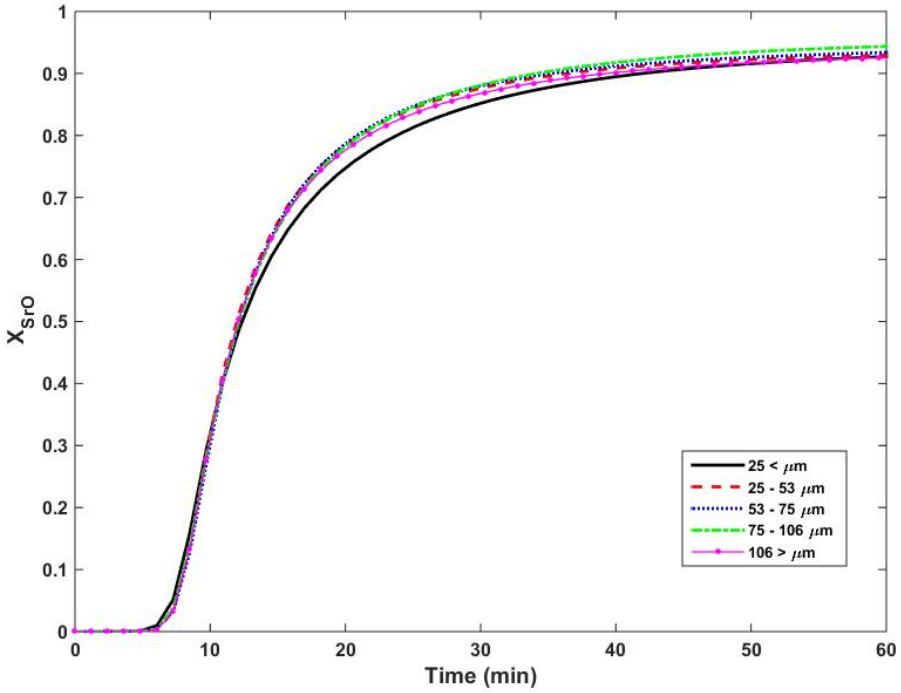

Figure 3 Isothermal kinetic curves of SrO carbonation at 1100 °C under CO2 pressure of 1 bar for different particle size

2.3. Operation of the carbonation reaction in a fixed bed reactor

Previously prepared SrO (25-106 µm), was mixed with sand (obtained from Avantor) (149 – 297 µm) as the dispersant, to avoid extreme built-up back pressure. Figure 4 shows a schematic of the laboratory scale apparatus designed and employed for strontium oxide carbonation. The experimental apparatus included a high temperature tube furnace (STT-1600C-2.5-4, Sentro Tech Corp.), and a real time gas analyzer (Hiden QGA, quantitative gas analyser). The material (mixture of 1 g SrO evenly dispersed in 4 g sand) was packed in the alumina tube with an internal diameter of

9.525 mm and kept in place with alumina insulation. Argon and CO_2 flowed through the system were separately monitored by two mass flow controllers.

During the first step, SrO was dehydrated at 1000 ºC under a continuous pure Ar flow at 0.2 slpm for 1 h. Temperature was then increased/decreased to the desired test temperature, and held at this temperature around 10 min to stabilize. In order to begin the carbonation reaction, the pure Ar flow gas was switched to the gas flow of 5% CO_2 and 95% Ar with the same total flow rate (0.2 slpm) as before. The carbonation reaction experiments were carried out at temperatures in the range of 900-1100ºC. The filtered, cooled exit stream was analyzed by a real time gas analyzer. In addition to the carbonation experiment explained above, empty runs were separately performed in the same experimental sequence to obtain the blank signal data using the tube furnace filled with only dispersant of the same bed size without SrO.

The CO_2 was correlated to a CO_2 volumetric flow rate by virtue of the known flow rate of inert gas and a calibration curve relation the ratio of gas signals to ratio of gas flowrates. The amount of CO_2 absorbed by SrO was calculated by subtracting the blank run signal data from the reaction run signal data.

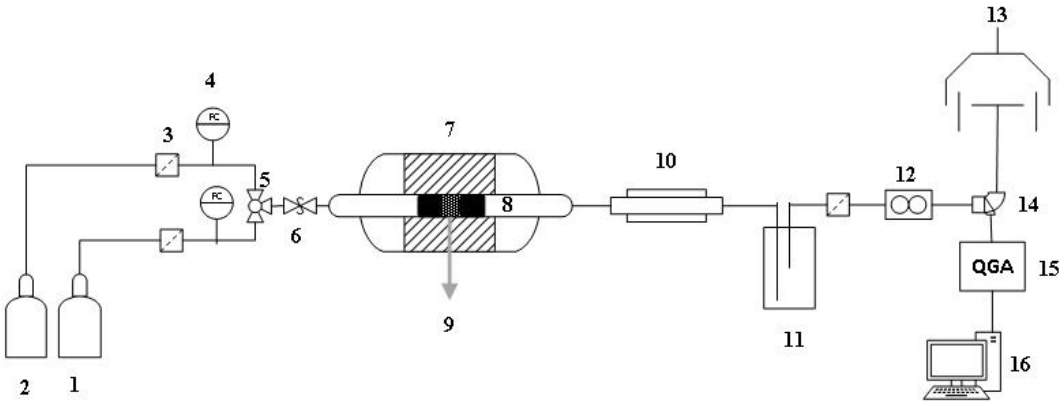

Figure 4 Schematic diagram of the fixed bed reactor system: (1) Argon cylinder, (2) CO_2 cylinder, (3) filter, (4) mass-flow controller, (5) 3-way plug valve, (6) pressure relief valve, (7) tube furnace, (8) insulation (9) SrO particle, (10) condenser, (11) silica gel, (12) mass flow meter, (13) extractor hood, (14) tee junction, (15) real time gas analyzer, (16) data acquisition system.

Depending on CO_2 flow rate, the amount of reactive material present, and temperature, CO_2 concentration at the exit would momentarily be zero because the material consumed all the CO_2 flowing through the bed. The CO_2 concentration in effluent gas begins to increase when the bed reaches saturation. This rapid change is called "breakthrough".[16]

The breakthrough curve of CO_2 capture is characterized by a variation of dimensionless concentration value (C/C_0) with time, where C and C_0 are CO_2 concentrations (mol/L) at the exit and entrance of the tube furnace, respectively. The conversion of SrO can be computed as:

$$X_{SrO} = \frac{M_{SrO}}{m_0} \int_0^t Q_g (C_0 - C) dt \qquad (5)$$

where X_{SrO} is the carbonation conversion of SrO, M_{SrO} is the molecular weight of SrO (g/mol), m_0 is the initial mass of SrO (g), Q_g is the gas flow (slpm).

3. Result and discussion

3.1. Thermogravimetric analysis

Figure 5 presents the fractional conversion versus time for carbonation of SrO at different carbonation temperatures ranging from 900°C to 1150°C with 1 bar CO_2 pressure.

Figure 5 shows similarly shaped kinetic curves. The carbonation reaction progression can be divided into three stages: an initial induction period; a rapid kinetically-controlled carbonation stage primarily on the surface of the sample; and finally a sluggish diffusion-controlled regime that takes place as CO_2 diffuses through a layer of $SrCO_3$ formed on the surface in the second stage. There is a quite abrupt transition between the initial induction period and rapid carbonation while the transition between the second and third stage takes more time. Final conversion is close to completion at temperatures higher than 900 °C but the complete conversion of SrO ($\alpha = 1$) is never reached due to diffusion limitation through the product layer and sintering.

Although lower temperature carbonation should theoretically have higher final reaction extent from thermodynamics, it is interesting to note that carbonation at higher temperature resulted in greater conversion after the given amount of time. Though these observations are in contrast to thermodynamic predictions, they agree well with previous work with CaO carbonation.[18,19] This is likely due to greater solid phase diffusional transport of CO_2 through the $SrCO_3$ product layer at higher temperature. Slow diffusion at lower temperature makes the ultimate conversion practically unachievable within reasonable time frames.

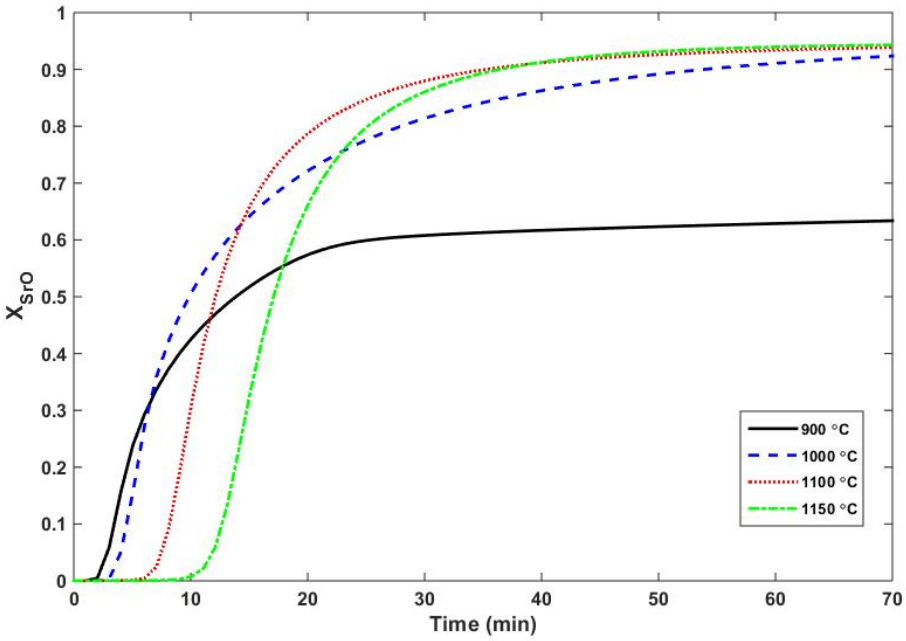

Figure 5 Isothermal kinetic curves of SrO carbonation under CO2 pressure of 1 bar

The effect of CO_2 pressure on carbonation was investigated by trials at 0.1, 0.25 and 1 bar CO_2. In the situations where the CO_2 was not 100%, nitrogen was used as the balance gas. Other parameters such as particle size (53-75 μm), and initial mass (~40 mg) were held constant. Each run was started with a fresh sample of heat-treated SrO. Figure 6 shows the effect of CO_2 partial pressure on carbonation at 900 °C and 1000 °C, respectively. P_{CO2} has a more dramatic effect at 1000 °C, whereas at 900 °C the effect is minimal. This can be explained by the thermodynamics, as the equilibrium P_{CO2} increases with the temperature.

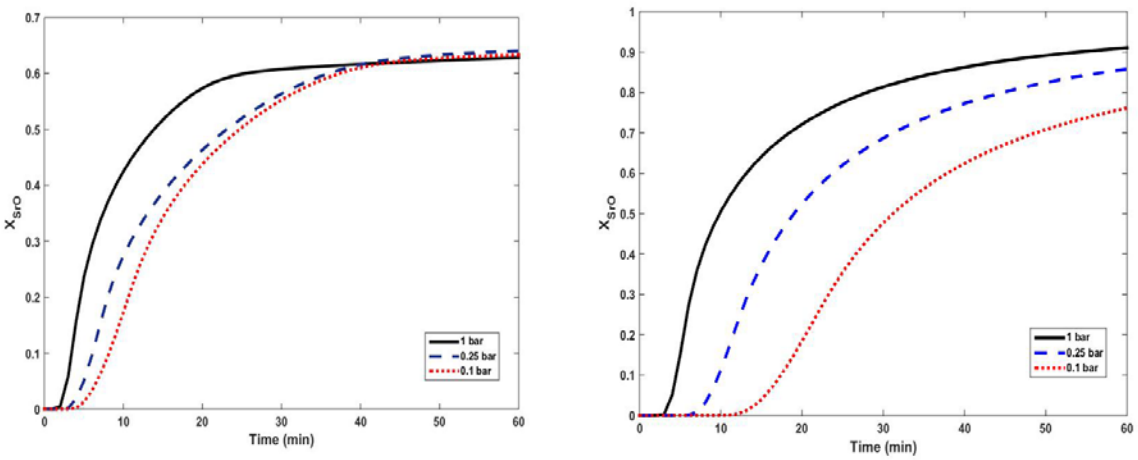

Figure 6 Isobaric kinetic curves of SrO carbonation at 900 °C (a) and 1000 °C (b)

The induction period refers to a period of time, sometimes several minutes, where a nucleation process must take place before a reaction can occur. Observation of this phenomena can be distorted if the experimental system has non-negligible "artifacts" such as time lag between actual reaction and the instrumentation tracking the reaction progress. The variation of this apparent induction period with the carbonation temperature is represented in Figure 7. The apparent induction time increases almost exponentially from 1 to 10 minutes with carbonation temperature in the range 900-1150°C. Conversely, Figure 6 shows that an apparent induction time decreases with an increase in CO_2 pressure. An apparent time is measured as the CO_2 starts to flow in TGA until the mass gain began to be greater than the thermobalance noise ($\Delta m > 1$ µg).

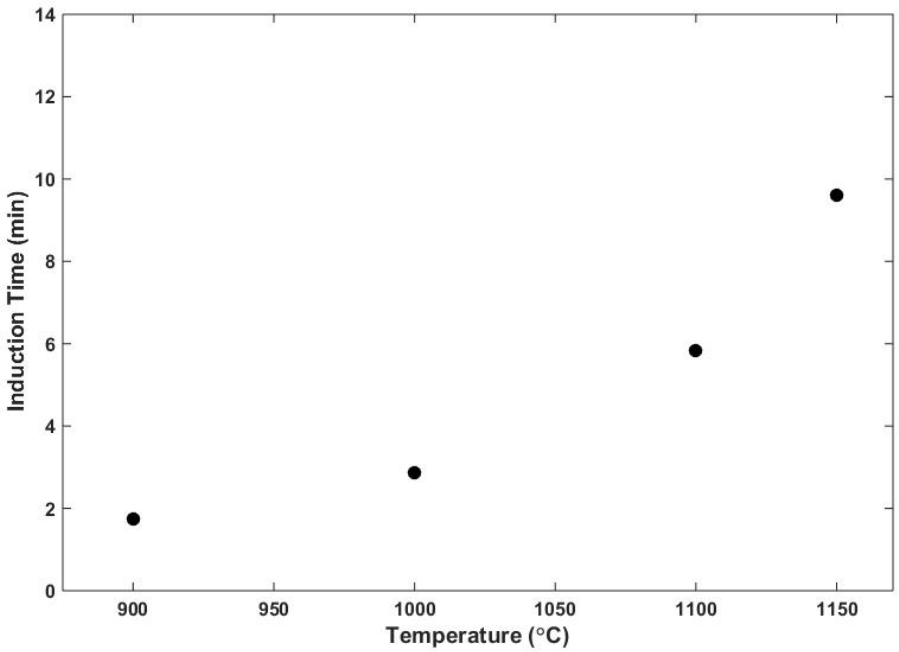

Figure 7 Apparent induction time versus temperature

The question of whether this is a true induction period versus a mere experimental artifact must be investigated in an experimental apparatus other than a TGA and is the subject of further study. As a kinetic model to account for the induction time is inappropriate at this stage, this time period was removed from conversion data. Figure 8 shows the fractional conversion versus time at different temperatures after removing the apparent induction period.

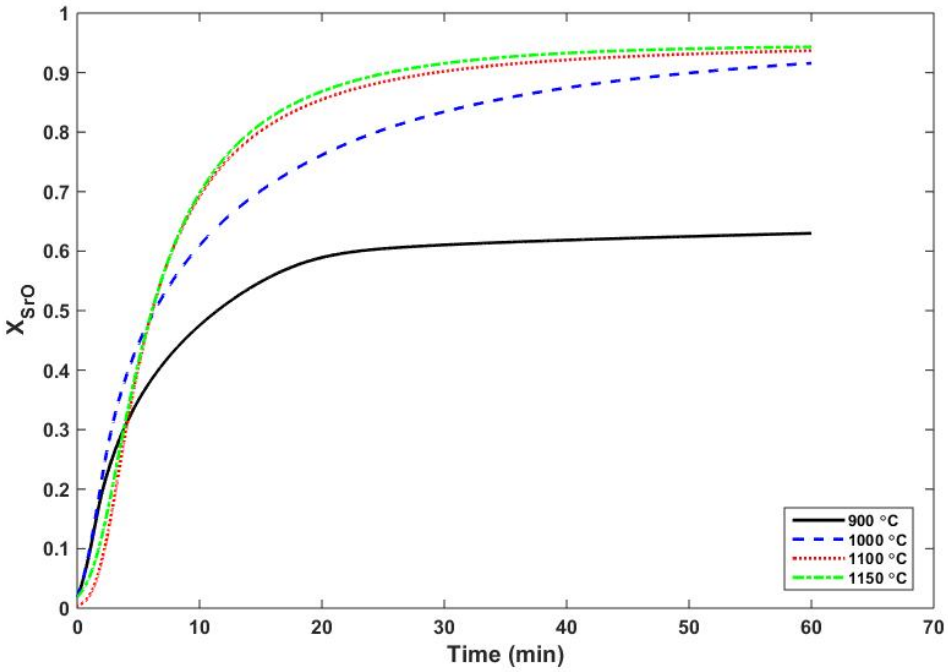

Figure 8 Isothermal kinetic curves of SrO carbonation under CO2 pressure of 1 bar after removing the apparent induction period

3.2. Fixed bed reactor

In this study, breakthrough curve analysis was conducted under different conditions. Figure 9 illustrates the concentration ratio (C/C_0) measured in the effluent gas versus time for different temperature between 900 and 1100 °C. Figure 10 displays the conversion of SrO as a function of time for different temperature calculated using equation (5).

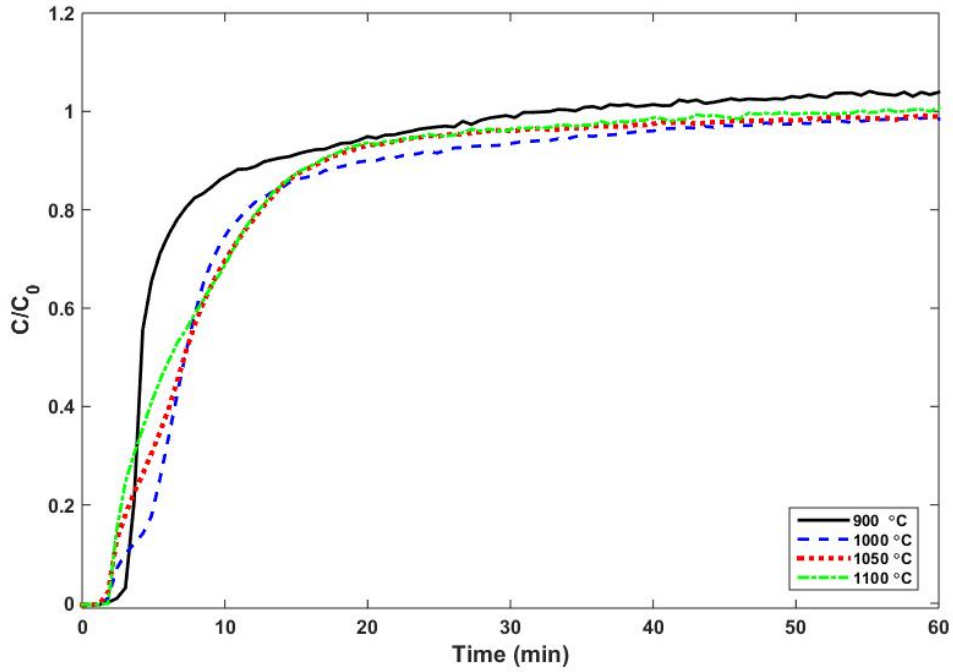

Figure 9 Breakthrough curves at different temperatures

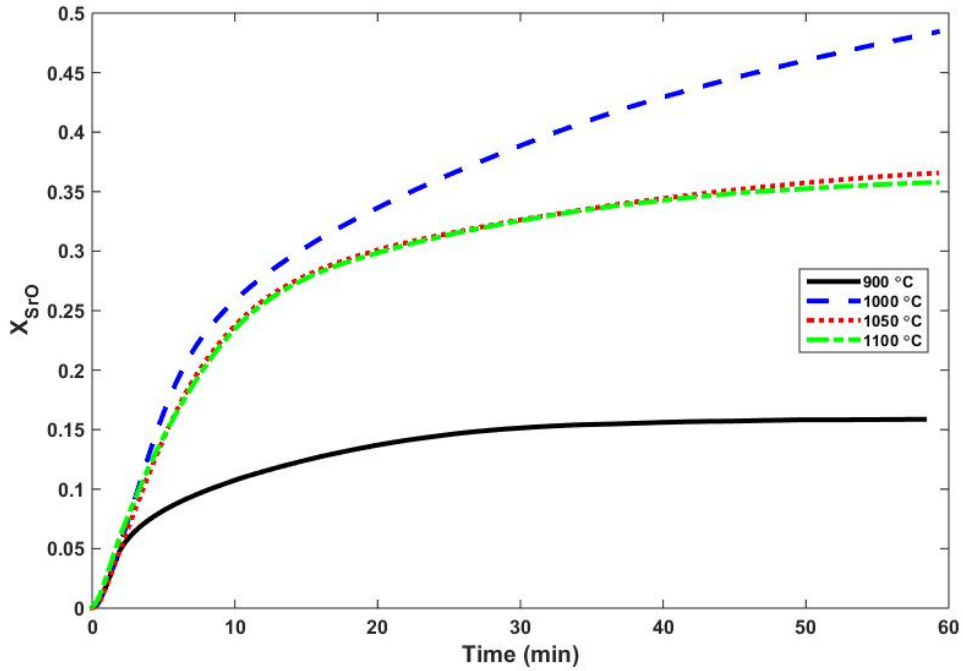

Figure 10 Conversion of SrO as a function of time

3.3. Kinetic Modeling

The kinetics of CaO carbonation have been heavily studied previously and several models have been presented.[19–23] The general consensus is that carbonation occurs in two consecutive rate controlling regimes: kinetic-controlled and diffusion-controlled. [16,21,24,25] In some cases, the induction period has been observed as well. [18,26] The kinetic-controlled regime is where the maximum rate of reaction is observed, and thus is the most relevant to understanding the intrinsic reaction rates. In the diffusion-limited regime, mass transfer limits the rate of reaction due to formation of a layer of product ($SrCO_3$) on the external surface of SrO particles. It is desired that the kinetic model describe both the kinetic and diffusion controlled regimes.

In contrast to many common processes where carbonation conversion often reaches completion within a few minutes, the ultimate fractional conversion of an alkali metal-based sorbent such as CaO or SrO, K_2CO_3 is usually limited to a value less than unity in the carbonation reaction due to the diffusion limitation of gaseous reactants through the outer solid product layer.[27] In order to describe such gas-solid reaction kinetic, various models have been introduced. Most classical are the continuous model and unreacted core model.[28] Bhatia and Permutter [19] developed random pore model as given below to correlate reaction behavior with internal pore structure in two regimes:

$$\frac{1}{\Psi}[\sqrt{1-\Psi \ln(1-X)}-1] = k't \qquad (6)$$

$$\frac{1}{\Psi}[\sqrt{1-\Psi\ln(1-X)}-1]=k''\sqrt{t} \qquad (7)$$

where Ψ is a structural parameter depending on the surface area, porosity, and the initial total length of pore system per unit volume, and k′ k″ are rate constant. Equation (6) is for chemical reaction control regime, and equation (7) for diffusion control regime. This model is informative for understanding the impact of structural parameters to determine the rate of carbonation reaction. However, this model is very complex to employ and determining the structural parameters is challenging.

Similar to CaO, the conversion curves of the SrO carbonation indicates a rapid rates at low conversion levels, with different initial rates depending on temperature. As the conversion increases to an ultimate conversion, X_u, at which no more significant conversion is attained at each temperature, the rate of carbonation approaches to zero. Lee's model,[21] which was developed on Bhatia and Permutters's data, is also applied to describe the apparent kinetics of CaO carbonation in two regimes. It is expressed by:

$$\frac{dX}{dt}=k(1-\frac{X}{X_u})^n \qquad (8)$$

where n is the reaction order X_u is the ultimate conversion when the rate of carbonation approaches zero. At the initial stage of carbonation reaction where the conversions are low, the rate of carbonation conversion is dependent on *k* in equation (8). Thus *k* can be regarded as the apparent chemical reaction rate. Integrating equation (8) yields:

for $n=1$:

$$X = X_u\left[1-\exp(-\frac{k}{X_u}t)\right] \qquad (9)$$

for $n=2$:

$$X = \frac{X_u t}{(X_u / k) + t} \qquad (10)$$

In equations (9) and (10), both k and X_u are a function of reaction temperature. Lee's model assumes that the effect of CO_2 partial pressure on the reaction rate is negligible. Least-square regression analysis has been conducted for equation (9) and (10) using the conversion data shown in Figure 8 and Figure 10 to compare their relative appropriateness for correlating the data. The poorest coefficient of determination, R^2, in regression with equation (9) for TGA data, is 0.98 for data at 1000 °C, while the best one with equation (10) is 0.96 for data at 1150 °C, suggesting that the conversion data can be more closely depicted by equation (9). Moreover, regression using equation (10) results in the estimation of X_u values to be more than unity.

The parameters in equation (8), k and X_u can be determined throughout the least-squares curve fitting for the conversion data with time. The reaction rate constant k can be represented as an Arrhenius equation.

Figure 11 shows the results of the least-squares regression fit to equation (9) of the carbonation conversion data experimented via TGA at temperature between 900ºC and 1150ºC and 100% CO_2. Table 3 lists determined parameter values for the carbonation reaction results conducted at different reaction temperatures.

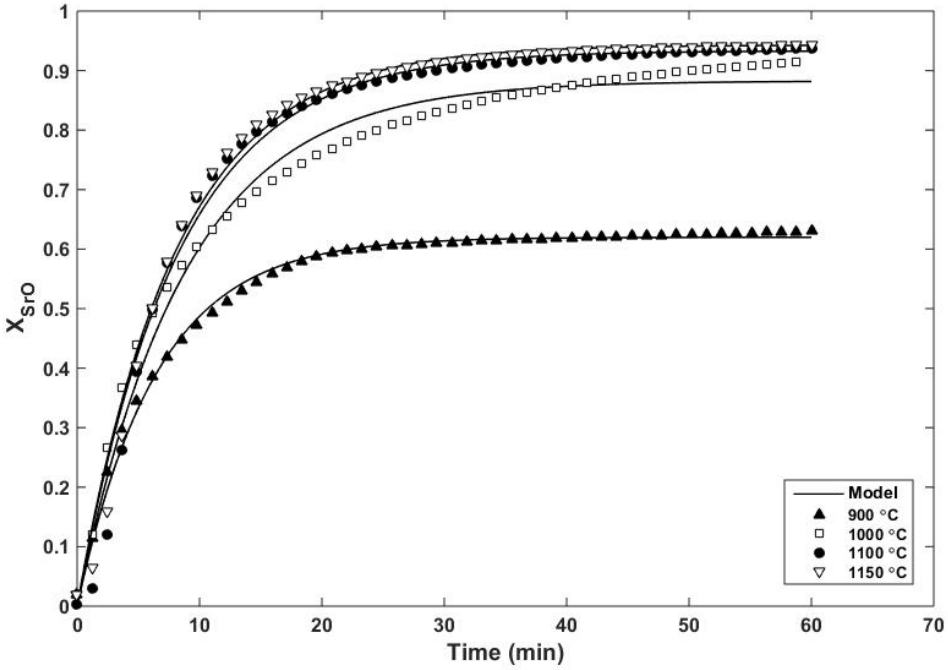

Figure 11 Least squares fit to equation (9) of the carbonation conversion data (TGA)

Table 3 Parameter values determined in the least squares fit of conversion data (TGA) to equation (9)

T, °C	X_u, -	k,1/min	R^2
900	0.62	0.0955	0.995
1000	0.88	0.1013	0.98
1100	0.93	0.1141	0.99
1150	0.94	0.1174	0.99

Figure 12 shows an Arrhenius plot. The apparent activation energy and pre-exponential factor obtained by linear fitting were: E_a = 12.01 kJ.mol^{-1} and A = 0.323 min^{-1} .

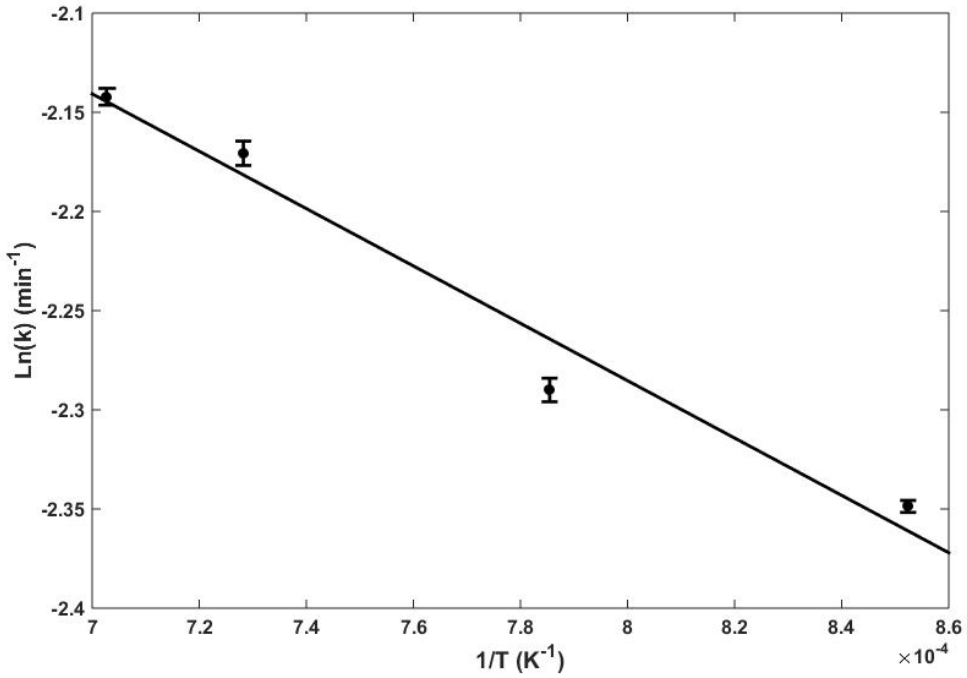

Figure 12 Determination of parameters of Arrhenius form of SrO carbonation (TGA)

The reaction rate constant *k* can be expressed as:

$$k = 0.323 \exp\left[-\frac{12018.7}{RT}\right] \qquad (11)$$

4. Conclusions

Concentrated solar power (CSP) in conjunction with thermal energy storage (TES) can reduce the use of fossil fuels and increase the utilization of solar energy by enabling plant operators to generate electricity beyond normal on-sun hours. Thermochemical energy storage (TCES) is a type of TES system based on a reversible reaction that potentially offers greater volumetric and gravimetric energy density than latent or sensible energy storage. Thermogravimetric analysis and a laboratory scale fixed bed reactor apparatus were used to study carbonation of SrO particles at several temperatures for thermochemical energy storage. The impacts of temperature, CO_2 partial pressure and particle size were studied. The particle size of SrO varying from less than 25 μm to more than 106 μm had almost no effect on the carbonation behavior. CO_2 partial pressure has a more dramatic effect at the higher temperature. Carbonation conversions appeared as sigmoid curves due to the initial retardation in the carbonation reaction rate. This kinetic behavior could be represented with good accuracy by the Lee's proposed kinetic model: $X=X_u\{1-\exp(-kt/X_u)\}$. Temperature dependency of the reaction rate constant k was represented by Arrhenius equation with activation energy of E_a = 12.02 kJ.mol^{-1} and the pre-exponential factor of A = 0.323 min^{-1} for TGA.

5. References

1. Müller-Steinhagen, H. & Trieb, F. Concentrating solar power - A review of the technology. *Q. R. Acad. Eng.* 43–50 (2004). doi:10.1126/science.1168539

2. Voorthuysen, E. H. M. Van, Du, E. H. & Van Voorthuysen, M. The promising perspective of concentrating solar power (CSP). *2005 Int. Conf. Futur. Power Syst.* 1–7 (2005). doi:10.1109/FPS.2005.204207

3. Stekli, J., Irwin, L. & Pitchumani, R. Technical challenges and opportunities for concentrating solar power with thermal energy storage. *J. Therm. Sci. Eng. Appl.* **5,** 021011 (2013).

4. Rhodes, N. R. *et al.* Solar Thermochemical Energy Storage Through Carbonation Cycles of $SrCO_3$ /SrO Supported on $SrZrO_3$. *ChemSusChem* n/a–n/a (2015). doi:10.1002/cssc.201501023

5. Pardo, P. *et al.* A review on high temperature thermochemical heat energy storage. *Renew. Sustain. Energy Rev.* **32,** 591–610 (2014).

6. Valverde, J. M., Sanchez-Jimenez, P. E. & Perez-Maqueda, L. A. High and stable CO2 capture capacity of natural limestone at Ca-looping conditions by heat pretreatment and recarbonation synergy. *Fuel* **123,** 79–85 (2014).

7. Edwards, S. E. B. & Materić, V. Calcium looping in solar power generation plants. *Sol. Energy* **86,** 2494–2503 (2012).

8. Wang, S., Yan, S., Ma, X. & Gong, J. Recent advances in capture of carbon dioxide using alkali-metal-based oxides. *Energy Environ. Sci.* **4,** 3805–3819 (2011).

9. Qin, C., Liu, W., An, H., Yin, J. & Feng, B. Fabrication of CaO-based sorbents for CO 2 capture by a mixing method. *Environ. Sci. Technol.* **46,** 1932–1939 (2012).

10. Liu, W. *et al.* Synthesis of sintering-resistant sorbents for CO2 capture. *Environ. Sci. Technol.* **44,** 3093–3097 (2010).

11. Arlt, W. & Wasserscheid, P. Storing and transporting energy, comprises e.g. using one-component system of A and B in a chemical reaction under heat absorption and removal of carbon dioxide to form an energy-rich compound B. (2011). at <http://www.google.com/patents/DE102010009543A1?cl=en>

12. Randhir, K. *et al. Experimental evaluation of sacrificial pore formation using graphite in SrO/SrCO3 system for solar thermochemical energy storage*.

13. Charsley, E. L., Earnest, C. M., Gallagher, P. K. & Richardson, M. J. Preliminary round-robin studies on the ICTAC certified reference materials for DTA - Barium carbonate and strontium carbonate. *J. Therm. Anal.* **40,** 1415–1422 (1993).

14. Robbins, S. a., Rupard, R. G., Weddle, B. J., Maull, T. R. & Gallagher, P. K. Some observations on the use of strontium carbonate as a temperature standard for DTA. *Thermochim. Acta* **269-270,** 43–49 (1995).

15. Ptáček, P. *et al.* The kinetics and mechanism of thermal decomposition of SrCO 3 polymorphs. *Ceram. Int.* **41,** 115–126 (2014).

16. Dou, B., Song, Y., Liu, Y. & Feng, C. High temperature CO2 capture using calcium oxide sorbent in a fixed-bed reactor. *J. Hazard. Mater.* **183,** 759–765 (2010).

17. Barin, I. *Thermochemical data of pure substances*. (VCH, 1995).

18. Rouchon, L., Favergeon, L. & Pijolat, M. Analysis of the kinetic slowing down during carbonation of CaO by CO 2. *J. Therm. Anal. Calorim.* **113,** 1145–1155 (2013).

19. Bhatia, S. K. & Perlmutter, D. D. Effect of the product layer on the kinetics of the CO2-lime reaction. *AIChE J.* **29,** 79–86 (1983).

20. Nikulshina, V., Gebald, C. & Steinfeld, a. CO2 capture from atmospheric air via consecutive CaO-carbonation and CaCO3-calcination cycles in a fluidized-bed solar reactor. *Chem. Eng. J.* **146,** 244–248 (2009).

21. Lee, D. An apparent kinetic model for the carbonation of calcium oxide by carbon dioxide. *Chem. Eng. J.* **100,** 71–77 (2004).

22. Zhou, Z., Xu, P., Xie, M., Cheng, Z. & Yuan, W. Modeling of the carbonation kinetics of a synthetic CaO-based sorbent. *Chem. Eng. Sci.* **95,** 283–290 (2013).

23. Bhatia, S.K. and Perlmutter, D. D. A random pore model for fluid-solid reactions 2 Diffusion and Transport effects.pdf. *AIChE Journal* **27,** 247–254 (1981).

24. Nikulshina, V., Galvez, M. E. & Steinfeld, A. Kinetic analysis of the carbonation reactions for the capture of CO2 from air via the Ca(OH)2-CaCO3-CaO solar thermochemical cycle. *Chem. Eng. J.* **129,** 75–83 (2007).

25. Nikulshina, V. & Steinfeld, a. CO2 capture from air via CaO-carbonation using a solar-driven fluidized bed reactor-Effect of temperature and water vapor concentration. *Chem. Eng. J.* **155,** 867–873 (2009).

26. Rouchon, L., Favergeon, L. & Pijolat, M. New kinetic model for the rapid step of calcium oxide carbonation by carbon dioxide. *J. Therm. Anal. Calorim.* **116,** 1181–1188 (2014).

27. Lee, D. K. *et al.* Kinetic expression for the carbonation reaction of K2CO 3/ZrO2 sorbent for CO2 capture. *Ind. Eng. Chem. Res.* **52,** 9323–9329 (2013).

28. Kunii, D. & Levenspiel, O. in *Fluidization Engineering* 480–489 (Wiley, 1969).

6. Appendix

6.1. BET result

Started: 11/9/2015 9:11:04AM

Completed: 11/9/2015 1:08:38PM

Report Time: 11/9/2015 10:41:34PM

Sample Mass: 0.4617 g

Cold Free Space: 84.5290 cm^3

Ambient Temperature: 22.00 °C

Automatic Degas: Yes

Analysis Adsorptive: N_2

Analysis Bath Temp: 77.317 K

Thermal Correction: Yes

Warm Free Space: 27.5194 cm^3 Entered Cold

Equilibration Interval: 45 s

Low Pressure Dose: 20.000 cm^3/g STP

Summary Report

Surface Area

BET Surface Area: 4.3427 m^2/g

BJH Adsorption cumulative surface area of pores between 17.000 Å and 3000.000 Å diameter: 3.089 m^2/g

Pore Volume

Single point desorption total pore volume of pores less than 1282.618 Å diameter at P/Po = 0.984813562: 0.024573 cm^3/g

BJH Adsorption cumulative volume of pores between 17.000 Å and 3000.000 Å diameter: 0.023054 cm^3/g

Pore Size

Desorption average pore width (4V/A by BET) :226.3379 Å

BJH Adsorption average pore diameter (4V/A): 298.481 Å

DFT Pore Size

Volume in Pores	<	23.41 Å	:	0.00074 cm^3/g
Total Volume in Pores	<=	4003.09 Å	:	0.02980 cm^3/g
Total Area in Pores	>=	23.41 Å	:	1.693 m^2/g